

Optical and Magneto-Optical Studies of Anomalous Anisotropy of the $\text{Cd}_{1-x}\text{Mn}_x\text{Te}$ Crystal

Liang-Yao Chen, Shi-Ming Zhou, Hong-Zhou Ma, Yi Su, and You-Hua Qian
T. D. Lee Physics Laboratory and Department of Physics, Fudan University
Shanghai, 200433, China

Chen-Jia Chen and Xue-Zhong Wang
Department of Physics, Peking University
Beijing, 100871, China

By using the magneto-optical and transmission-ellipsometric methods, giant anisotropy in both optical and magneto-optical properties was found for the single crystal $\text{Cd}_{1-x}\text{Mn}_x\text{Te}$ ($x=0.45$). Two orthogonal axes, E_{\perp} and E_{\parallel} , were in the (113) plane, and along the $[\bar{4}7\bar{1}]$ and $[21\bar{1}]$ directions, respectively. Both transmission-ellipsometric and magneto-optic Faraday rotation spectra located peaks at the same about 2-eV E_{Mn} position, that was in the gap between the conduction and valence bands. In discussion, E_{Mn} was attributed to the optical transition of $\text{Te } p \rightarrow \text{Mn } d_{\downarrow}$, and several possible mechanisms for the anisotropy phenomena were suggested and studied. A general and analytical equation was given to calculate the anomalous anisotropy of the Faraday effect, showing good agreement with experimental results. The equation can be used to explain other magneto-optical anisotropic properties of the system. The detailed results were given.

Among the Mn-doped II-VI magnetic semiconductor groups, $\text{Cd}_{1-x}\text{Mn}_x\text{Te}$ is probably the one that has been studied most extensively. It can be crystallized in a single-phase zinc-blende (ZB) structure up to a composition of $x=0.77$.¹ The free Mn atom has a $3d^5 4s^2$ configuration; hence, after doping the divalent Mn can replace Cd at the lattice sites. The behavior of the $3d^5$ electrons of Mn^{2+} with their spin parallel (up) by Hund's rule plays a significant role, resulting in such a property as the giant Faraday rotation observed even at room temperature with a moderated magnetic field.² The pinning of the lowest excited energy level at ~ 2 eV above the Γ_8 valence band as $x \geq 0.4$ is another interesting phenomenon^{3,4}, and is now attributed more likely to a $\text{Mn}^{2+} 3d^5$ intraband transition of ${}^6A_1 \rightarrow {}^4T_1$ with a spin flip in the band.⁵ This implies that the $3d^5$ ground state is close to the Γ_8 maximum, which is also indicated by band structure calculations of $\text{Cd}_{1-x}\text{Mn}_x\text{Te}$.⁶ Photoemission results,^{7,8} however, located the $3d^5$ band lying ~ 3.5 eV below Γ_8 . The experiment results seem to be undisputable, leaving only the interpretation in controversy. So further effort should be made to understand the role of Mn^{2+} better. It is usually thought that the Cd cations, which are arranged in an fcc sub-lattice of ZB structure, are randomly replaced by Mn^{2+} .¹ The $\text{Cd}_{1-x}\text{Mn}_x\text{Te}$ crystal has a high-temperature paramagnetic phase;⁹ therefore, at room temperature and zero field, the crystal should be macro-isotropic. Recently, however, as we studied the magneto-optical properties of $\text{Cd}_{1-x}\text{Mn}_x\text{Te}$ with $x=0.45$, we observed a giant optical and magneto-optical anisotropy existed in the crystal. We report this phenomena here.

Single crystal $\text{Cd}_{1-x}\text{Mn}_x\text{Te}$ with $x=0.45$, showing a uniform reddish color, was prepared by the

modified Bridgman method without special heat treatment. The sample was cut to a thickness of about 1.8 mm from the ingot section, and was polished and etched on both sides. The crystal is however brittle and can be cleft along some orientations. The x-ray diffraction data indicated that the polished and the side-cleft planes have the {113} and {110} index, respectively, as shown in Fig. 1. The spectra of the dielectric function measured by ellipsometry were in agreement with other results¹⁰. The fundamental absorption gap E_0 is at about 2.125 eV which is corresponds to the Mn composition of $x=0.45$ as was confirmed by the X-ray data.

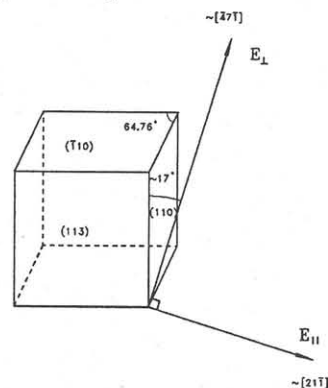


Fig. 1. The orthogonal E_{\perp} and E_{\parallel} orientations, are in the (113) plane, and along the $[\bar{4}7\bar{1}]$ and $[21\bar{1}]$ direction, respectively. $[113]$ is normal to the plane of the paper.

A rotating analyzer type of Kerr apparatus¹¹ was used to measure absolutely the spectra of the doubled pole Faraday rotation θ_F at room temperature by coating an Al film on the back side of the sample. The incident angle was about 2° . The linear-

polarization direction s of the incident beam was fixed and was perpendicular to the plane of incidence. We found that not only the hysteresis loop, which had zero coercivity, but also the Faraday spectra were strongly dependent on crystal orientation. At zero magnetic field, the pure cosine raw light-signal, was phase-shifted by a large value ϕ_0 for some orientations. This would not be the situation for a sample in a paramagnetic state, for example a glass plate. This meant that a giant zero-field rotation existed for the sample. As the field H was scanned from 0 to 10 KOe in the two opposite directions, θ_F did not vary linearly with H , and was dependent on both the photon energy E and sample orientation.

To understand this phenomena, we then used the angle-variable scanning ellipsometer¹² to measure the polarization states of transmittance by setting a 90° incidence angle with the incident beam being normal to the sample surface. In the system configuration, the azimuthal angle of the polarizer P_0 (in the s direction) was fixed and perpendicular to the incident plane to eliminate the residue polarization effect of the light source. The azimuthal angles P and A are those of the the polarizer and analyzer, respectively, and were initially zero with respect to the s axis. The polarizer and analyzer were synchronously rotated at different rate of $A=2P=\omega_0 t$, controlled by two micro-stepping motors having 10000 steps per revolution. If the sample were transparent and optically isotropic, inserting the sample would give the same result. If the sample is not optically isotropic, however, linearly polarized light will emerge from the sample in an elliptically polarized state. This is the case with $\text{Cd}_{1-x}\text{Mn}_x\text{Te}$ ($x=0.45$) as can be seen in Fig. 2 where the results for the sample and air are compared. The sample has two special orientations, E_\perp and E_\parallel , lying in the (113) plane and perpendicular to each other, as indicated in Fig. 1. The results show clearly that $\text{Cd}_{1-x}\text{Mn}_x\text{Te}$ ($x=0.45$) is optically anisotropic.

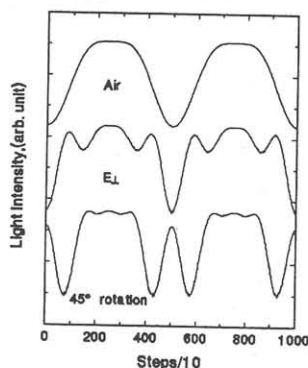


Fig. 2. The raw data were measured by a transmittance ellipsometer at 2 eV for air, and the sample as $E_\perp \parallel s$ and rotating 45° from E_\perp direction, respectively, and showed clearly the anisotropy.

Next, we scanned the photon energy in the 1.5-2.3 eV range with a 0.01-eV interval to determine Ψ and Δ by setting E_\perp and E_\parallel be along the s axis, respectively. The spectra of Ψ and Δ are shown in Fig. 3. The two curves for Ψ_\perp and Ψ_\parallel are nearly mirror-

reflected by the line of $\Psi=45^\circ$. Since $\cos\Delta$ is an even function, there is a sign uncertainty in Δ , so we give the Δ spectra without sign in the figure to show that the magnitudes of Δ_\perp and Δ_\parallel are consistent. The large values of Δ ($> 100^\circ$ in zero order) implies that the crystal has different dispersion features, i.e., there are two refractive indexes, n_\perp and n_\parallel , corresponding to the E_\perp and E_\parallel orientation, respectively. The sharp peaks for both Ψ and Δ spectra are located exactly at 2.07 eV.

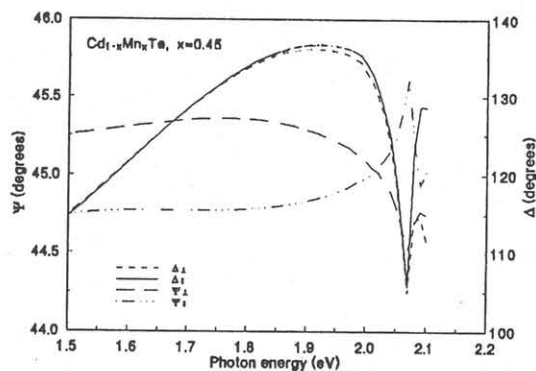


Fig. 3. Spectra of Ψ and Δ were measured by the ellipsometer, and showed sharp peaks at 2.07 eV.

Once the orientations of the crystal were determined, we measured the Faraday data again. We found that when either the E_\perp or E_\parallel orientation was parallel to the s direction, the zero-field phase-shift ϕ_0 was nearly zero, and $\theta_{F\perp}$ and $\theta_{F\parallel}$ were small. When the sample was rotated about 45° , ϕ_0 and $\theta_F^{45^\circ}$ were both maximum. $\theta_F^{45^\circ}$ was about 10 times larger than $\theta_F^{E_\perp}$. The spectra of $\theta_F^{45^\circ}$ measured under different magnetic fields were shown in Fig. 4. The hysteresis loops of $\theta_{F\perp}$, θ_F and $\theta_F^{45^\circ}$ were anti-symmetric and were not exactly linear to the magnetic field H as shown in the top insert of Fig. 4. In other crystal orientations, the loops were not anti-symmetric to H . Comparing the 2.07-eV peaks of Ψ and Δ at zero field in Fig. 3, the peaks of the θ_F spectra were located around 2 eV, and were red-shifted with increasing field. We attribute this structure, say E_{Mn} , to the same origin of the 2-eV pinning level as observed in other experiments,^{3,4} and that is clearly due to Mn^{2+} .

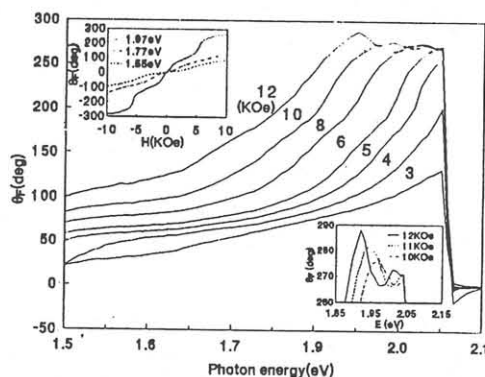


Fig. 4. Spectra of Faraday rotation $\theta_F^{45^\circ}$ were measured when E_\perp axis was rotated 45° from the s direction. In the bottom insert double peaks are shown.

The giant Faraday rotation of Mn-doped II-VI magnetic semiconductors has been suggested to be due to enhanced Zeeman splitting of the conduction and valence bands with the maximum of θ_F occurring when the photon energy was equal to E_o .^{13,14} The peaks of θ_F spectra in Fig. 4, however, were clearly related to E_{Mn} , not to E_o (2.125 eV). Detailed theoretical calculations of $Cd_{1-x}Mn_xTe$ ⁶ suggested that there are two sets of energy levels near Γ_8 with the gaps being close enough to each other to be involved in the transition at ~ 2.0 eV, i.e., the $d^5 \rightarrow d^{5*}$ transition ($6A_1 \rightarrow 4T_1$, $\Delta E \sim 2.2$ eV), and the Te $p \rightarrow Mn d_{\downarrow}$ transition ($\Delta E \sim 2.0$ eV). By the optical-transition selection rules of $\Delta l = \pm 1$, $\Delta m_l = \pm 1$, and $\Delta S_z = \pm 1$,¹⁵ where l , m_l and S_z are the quantum numbers corresponding to orbital momentum, and the Z component of orbital momentum and spin, respectively, the $d^5 \rightarrow d^{5*}$ transition will be less expected than the Te $p \rightarrow Mn d_{\downarrow}$ transition. We also notice that the calculated gap value for the latter transition is in remarkable agreement with our measured value, though the selection rules could be relaxed due to a mixture of $Mn^{2+} 3d^5$ states in part with the s and p states of Te and Cd. The fundamental transition ($\Gamma_8 \rightarrow \Gamma_6$) was mainly related to the s-p states. It was well known, however, that magneto-optical transitions are favored by the "magnetic electrons", i.e., d states in the transition metals and d and f states in the rare-earth metals, and strongly discriminate against s-p states due to dependence on the spin-orbit coupling strength.¹⁶ The giant Faraday rotation will be cut off at E_o in the cases of either $E_o > E_{Mn}$ or $E_o < E_{Mn}$ due to the fundamental absorption being ~ 20 times stronger than the absorption at E_{Mn} ,¹⁷ as clearly observed in this and other experiments although different interpretations have been given.^{13,14,18}

Unlike the Mn-doped II-VI magnetic semiconductors with a hexagonal wurtzite structure, such as $Cd_{1-x}Mn_xSe$,¹⁹ which has an intrinsic birefringence and causes the optical and magneto-optical properties to be anisotropic, the $Cd_{1-x}Mn_xTe$ crystals ($x < 0.77$) have a ZB structure and should be both optically and magneto-optically isotropic. We have shown in this work that $Cd_{1-x}Mn_xTe$ with $x = 0.45$ has anisotropic feature. The origin of this giant anisotropy is under study, and may be from the possible residual stress, arising from the effects of non-uniform alloy concentration and thermal gradient when the crystal was grown, or from the orderly-distributed magnetic atoms which cause lattice distortion to make the anisotropy occur along special crystal orientations. The similar phenomena of order-disorder transitions were also found in the GeSi alloy system.

After studies, we found that for a general case the experimentally measured Faraday rotation ψ for a magneto-optical anisotropy system will be different from ordinary one, and can be given as:

$$\tan 2\psi =$$

$$\frac{\sin 2\theta \cos \delta - \cos 2\theta \sin 2\alpha \sin \delta}{\cos 2\theta (\cos^2 2\alpha + \sin^2 2\alpha \cos \delta) + \sin 2\theta \sin 2\alpha \sin \delta}$$

where, θ is the azimuthal angle of the linearly-polarized incident light, α and δ are two parameters related to the optical and magneto-optical anisotropy of the material structures. For an isotropic system, $\alpha = 45^\circ$ and $\delta = 2\theta_F$, where θ_F is the true Faraday rotation angle defined in the literature. In terms of the equation, we have calculated the Faraday rotation by fitting the two parameters and obtained the results in good agreement with experimental data which will be discussed in more detail and published elsewhere.

In conclusion, by using magneto-optical and transmission ellipsometric methods, the giant optical and magneto-optical anisotropy of single crystal $Cd_{1-x}Mn_xTe$ ($x = 0.45$) were shown. Both ellipsometric and magneto-optic Faraday rotation spectra located the peaks at the same E_{Mn} position, that was clearly in the gap between the conduction and valence bands and was attributed to the optical transition of Te $p \rightarrow Mn d_{\downarrow}$. A general and analytical equation was given to explain other magneto-optical anisotropic properties of the system. A better understanding of the anisotropy of $Cd_{1-x}Mn_xTe$ may reveal further how Mn^{2+} influences the crystal properties.

This work was supported by SSTC, SEC, and NSF of China.

References

1. J. K Furdyna, J. Appl. Phys. **64**, R29 (1988).
2. A. E. Turner, R. L. Gunshor, and S. Datta, Appl. Opt. **22**, 3152 (1983).
3. P. Lemasson, B. L. Wu, R. Triboulet, and J. Gautron, Solid State Commun. **47**, 669 (1983).
4. Y. R. Lee and A. K. Ramdas, Solid State Commun. **51**, 861 (1984).
5. Y. R. Lee, A. K. Ramadas, and R. L. Aggarwal, Phys. Rev. B **33**, 7383 (1986).
6. S. H. Wei and A. Zunger, Phys. Rev. B **35**, 2340 (1987).
7. A. Franciosi, S. Chang, R. Reifenberger, U. Debska, and R. Riedel, Phys. Rev. B **32**, 6682 (1985).
8. M. Taniguchi, L. Ley, R. L. Johnson, J. Ghijsen, and M. Cardona, Phys. Rev. B **33**, 1206 (1986).
9. B. E. Larson, K. C. Hass, and R. L. Aggarwal, Phys. Rev. B **33**, 1789 (1986).
10. P. Lautenschlager, S. Logothetidis, L. Viññ, and M. Cardona, Phys. Rev. B **32**, 3811 (1985).
11. L. Y. Chen and J. Woolam, Proc. of SPIE Symposium, **1166**, 267 (1989).
12. L. Y. Chen, X. W. Feng, Y. Su, H. Z. Ma, and Y. H. Qian, Appl. Opt., in press, 1993.
13. D. U. Bartholomew, J. K. Furdyna, and A. K. Ramdas, Phys. Rev. B **34**, 6943 (1986).
14. H. J. Jimenez-Gonzalez, R. L. Aggarwal, and P. Becla, Phys. Rev. B **45**, 14011 (1992).
15. J. L. Erskine and E. A. Stern, Phys. Rev. B **8**, 1239 (1973).
16. J. L. Erskine and E. A. Stern, Phys. Rev. Lett. **30**, 1329 (1973).
17. M. E. Amezian, J. P. Lascaray, and J. Diouri, Solid State Commun. **45**, 351 (1983).
18. J. A. Gaj, R. R. Gatazka, and M. Nawrocki, Solid State Commun. **25**, 193 (1978).